

Fermi-surface-topology tuned high temperature superconductivity in the cuprates

N. Harrison, R.D. McDonald, and J. Singleton

National High Magnetic Field Laboratory, Los Alamos National Laboratory, MS E536, Los Alamos, New Mexico 87545

(Dated: September 5, 2021)

Based on recent magnetic-quantum-oscillation, ARPES, neutron-scattering and resistivity data, we propose that the extraordinarily high superconducting transition temperatures in the cuprates are driven by an exact mapping of the incommensurate spin fluctuations onto the $d_{x^2-y^2}$ Cooper-pair wavefunction. Strong evidence for this comes from the direct correspondence between the incommensurability factor δ seen in inelastic neutron scattering and the inverse superconducting coherence length (see Fig. 2). Based on these findings, one can specify the optimal characteristics of a solid that will exhibit “high T_c ” superconductivity.

In spite of strong evidence for an order parameter exhibiting $d_{x^2-y^2}$ symmetry [1] in the “High T_c ” cuprate superconductors, experiments establishing a direct link with the pairing mechanism have not been forthcoming. However, with the advent of magnetic-quantum-oscillation measurements on underdoped cuprates [2, 3, 4] and consequent proposals for the Fermi-surface topology that are consistent with experiments ranging from neutron scattering to ARPES [4, 5, 6], there is the opportunity to resolve this issue. We find that the $d_{x^2-y^2}$ Cooper-pair wavefunction is exactly tuned to the real-space form of the fluctuations responsible for the incommensurate antiferromagnetic scattering observed in inelastic neutron experiments on all doped cuprates [7, 8, 9, 10, 11, 12] (see e.g. Fig. 1a). The dispersion of these fluctuations, which are likely to be driven by the varying topology of the Fermi surface as the hole density p increases [4], provides a very plausible energy scale for T_c in the cuprates [8].

Most treatments of superconductivity consider the state as a condensate [13, 14, 15, 16, 17]; in such a picture, it is natural to treat the Cooper-pair wavefunction in k -space. However, we are interested in the similarity of the spatial distribution of spin-fluctuations and the Cooper pair, and so we consider the form of the two-dimensional $d_{x^2-y^2}$ Cooper-pair wavefunction in real space [1, 17]:

$$\psi(\mathbf{r}) \propto \cos(rk_F)(x^2 - y^2)e^{-3r/\xi_0}. \quad (1)$$

Here $r = \sqrt{x^2 + y^2}$ is the cylindrical polar radius, x and y are corresponding Cartesian coordinates, k_F is the Fermi wavevector [2, 3] and ξ_0 is the superconducting coherence length. Figure 1(b) shows a contour plot of $\psi(\mathbf{r})$; the known diagonal nodal regions [1, 16] are clearly visible. In such a plot, the lengthscale over which $\psi(\mathbf{r})$ is non-negligible is defined by ξ_0 (Eq. 1). We now consider similarities between this wavefunction and the real-space topology of the incommensurate antiferromagnetic fluctuations seen in inelastic neutron scattering [7, 8, 9, 10, 11, 12].

Low-energy inelastic neutron-scattering data for both $\text{La}_{2-x}\text{Sr}_x\text{CuO}_4$ [9, 12] and $\text{YBa}_2\text{Cu}_3\text{O}_{7-x}$ [10, 11] follow

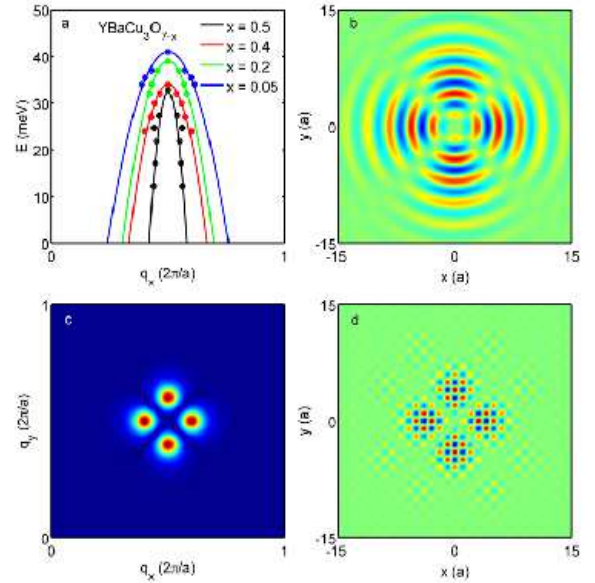


FIG. 1: (a) Energy (E) versus q_x for several $\text{YBa}_2\text{Cu}_3\text{O}_{7-x}$ compositions [10, 11], with fits to Eq. 2 to obtain extrapolated values of δ at $E = 2$ meV (dotted line). (b) Contour plot of d -wave Cooper-pair wavefunction in two-dimensions (Eq. 1); we assume a Fermi wavevector $k_F = \pi/\sqrt{2}a$ where a is the lattice parameter, while $p = 0.1$ for which we select $\xi_0 = 27$ Å from Table I. (c) Simulation of the incommensurate neutron scattering peaks obtained by Fourier transforming Eq. 3; δ and ξ correspond to $p = 0.1$ (Table I). (d) Real-space spin-fluctuation map corresponding to the set of four incommensurate peaks in (b), also for $p = 0.1$ (see Table I). We consider the simple case where $s_{\mathbf{Q}}$ is the same for all \mathbf{Q} .

an approximately inverted parabolic form

$$E(\mathbf{q}) = E_0 \left(1 - \frac{a^2(\mathbf{q} - \mathbf{Q}_0)^2}{\pi^2 \delta^2} \right), \quad (2)$$

where a is the in-plane lattice parameter and E_0 is a doping-dependent energy scale [7, 8, 9, 10, 11]; some examples are shown in Fig. 1(a). Here, δ depends on the composition and doping of the cuprate involved [7, 8, 18]; some values are given in Table I. As $E \rightarrow 0$, the brightest scattering intensity typically appears at a cluster of four

incommensurate peaks at $\mathbf{Q} = (\pm\pi/a, \pm(1\pm 2\delta)\pi/a)$ and $(\pm(1\pm 2\delta)\pi/a, \pm\pi/a)$ [7, 8, 9, 10, 11, 12]; a simulation is shown in the positive q_x , positive q_y quadrant of two-dimensional k -space in Fig. 1(c). The form of the scattering peaks in Fig. 1(c) is already very suggestive of the $d_{x^2-y^2}$ wavefunction in Fig. 1(b); to make a quantitative comparison, however, we require a real-space representation of the corresponding spin fluctuations.

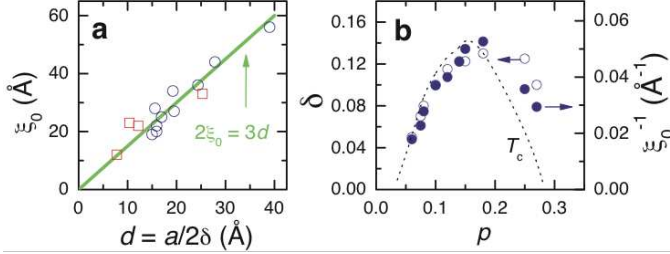


FIG. 2: **a** The approximately linear correspondence between $d = a/2\delta$ and ξ_0 for $\text{La}_{2-x}\text{Sr}_x\text{CuO}_4$ (\circ) and $\text{YBa}_2\text{Cu}_3\text{O}_{7-x}$ (\square). The line represents the ratio $\xi_0/d = 3/2$. **b** Plot showing δ and ξ_0^{-1} in $\text{La}_{2-x}\text{Sr}_x\text{CuO}_4$ exhibiting a maximum versus p in a similar fashion to T_c (scaled for comparison), though T_c falls more rapidly with p beyond optimal doping.

A simple model of spin fluctuations that can produce the observed incommensurate scattering peaks is a sinusoidal variation of the staggered moment modulated by an exponential damping factor; the latter term represents the fact that the antiferromagnetic fluctuations possess a finite correlation length ξ [7, 18]. The spatially-varying moment is thus

$$s(\mathbf{r}, t) = \sum_{\mathbf{Q}} s_{\mathbf{Q}} \exp\left(-\frac{r}{\xi} + i\omega t\right) \cos(\mathbf{Q} \cdot (\mathbf{r} - \mathbf{r}_0)), \quad (3)$$

where ω is the angular frequency of the fluctuations, $\mathbf{r}_0 = (\pm d, 0)$ or $(0, \pm d)$ with $d = a/2\delta$, and the sum in \mathbf{Q} runs over the values given above. The simulation shown in Fig. 1(c) is a Fourier transform of Eq. 3 that reproduces the general form of the experimental neutron data [7, 8, 9, 10, 11, 12] very well. Note that the choice of \mathbf{r}_0 is quite critical; any other value would give significant intensity at $\mathbf{q} = \mathbf{Q}_0$, at variance with the experimental spectra. This is an important point, to which we will return. Finally, Fig. 1(d) shows a time-averaged contour plot of Eq. 3. The similarity between the spin fluctuation distribution and the $d_{x^2-y^2}$ wavefunction (Fig. 1(b)) is most marked: both show similar angular and radial distributions. Less obvious, but equally germane, is the phase of each function plotted. The choice of \mathbf{r}_0 necessary to reproduce the neutron data means that there is a π difference of phase between adjacent lobes of the spin-fluctuation distribution, just as there is a π difference in phase between adjacent lobes of the $d_{x^2-y^2}$ Cooper-pair wavefunction [1, 16].

As mentioned above, the lengthscale of the Cooper-pair wavefunction is ξ_0 ; the corresponding lengthscale

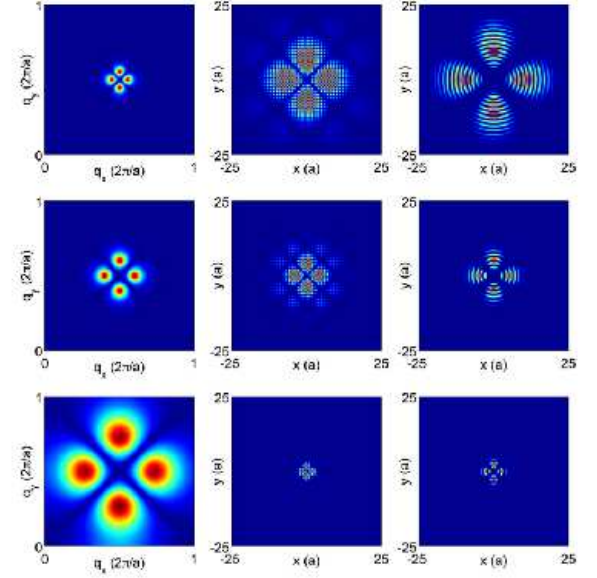


FIG. 3: Comparisons of the spin density amplitude and $d_{x^2-y^2}$ wavefunction at selected values of p . The first column shows plots of the incommensurate diffraction peaks obtained on re-Fourier transforming $s(\mathbf{r})$ calculated using Eq. 3 and the published values of δ and ξ listed in Table I. The second column shows the calculated $|s(\mathbf{r})|$ while the third column shows $\rho_c(\mathbf{r}) = |\Psi(\mathbf{r})|^2$ calculated according to the values of ξ_0 listed in Table I. Rows 1, 2 and 3 consecutively correspond to $p \approx 0.06, 0.1$ and 0.152 .

for the spin fluctuation distribution (Eq. 3) is $d = a/2\delta$ [7, 8, 9, 10, 11]. To further establish the causal relationship between the spin fluctuations and the superconducting pairing mechanism, we now compare independent estimates of these lengthscales for several cuprates. The values of d are obtained from inelastic neutron-scattering experiments. In the $\text{La}_{2-x}\text{Ca}_x\text{CuO}_4$ cuprates, the dispersion relationships (Fig. 1(b)) have been measured down to low energies, providing accurate values of δ [9]. However, there is a loss of intensity at lower energy transfers in $\text{YBa}_2\text{Cu}_3\text{O}_{7-x}$, possibly because of their greater homogeneity [10, 11], necessitating a downward extrapolation of the dispersion curves to obtain δ in the limit $E \rightarrow 0$. The coherence lengths ξ_0 are independently derived from magnetoresistance and other data [19, 20]; occasionally some interpolation is required to obtain values for the same hole doping and composition as the neutron-scattering data. Fig. 2a shows the corresponding values of ξ_0 plotted against d . Table I lists the values (plotted against doping for $\text{La}_{2-x}\text{Sr}_x\text{CuO}_4$ in Fig. 2b).

Remarkably, Fig. 2a shows that the ξ_0 versus d values for *all* compositions and dopings listed in Table I lie on a single straight line $\xi_0/d = 3/2$, irrespective of whether $\text{La}_{2-x}\text{Sr}_x\text{CuO}_4$ or $\text{YBa}_2\text{Cu}_3\text{O}_{7-x}$ is considered, suggesting a common origin for the spin fluctuations and the

superconductivity in all of the cuprates.

Having established the experimental relationship between ξ_0 and d , we can now plot the evolution with increasing hole density p of the spatial distribution of the spin fluctuations (Eq. 3) alongside the corresponding Cooper-pair wavefunction (Eq. 1) using experimental values of both parameters; Fig. 3 shows the result. At small values of p , the incommensurate neutron-scattering peaks occupy a small area of k -space [9, 10, 11]; the corresponding real-space spin fluctuation distribution occupies a large area, as does the Cooper-pair wavefunction. As p increases, the incommensurate peaks spread out in k -space [9, 10, 11]; hence, the spin-fluctuation spatial distribution is compressed, as is the Cooper-pair wavefunction.

TABLE I: Parameters for various cuprate superconductors, including hole doping p . For $\text{La}_{2-x}\text{Sr}_x\text{CuO}_4$, δ values measured at neutron transfer energies of $E \approx 2$ -3 meV are taken from Refs. [9, 12]. For $\text{YBa}_2\text{Cu}_3\text{O}_{7-x}$, δ values at the equivalent energy are taken from plots such as Fig. 2a using data from Refs. [10, 11]. Correlation lengths ξ are taken from Ref. [7] while BCS coherence lengths ξ_0 are taken from Refs. [19, 20], occasionally requiring interpolation between adjacent compositions for precise doping matches to δ .

compound	p	δ	ξ (Å)	ξ_0 (Å)	T_c (K)
$\text{La}_{1.94}\text{Sr}_{0.06}\text{CuO}_4$	0.06	0.05	17	56	13
$\text{La}_{1.925}\text{Sr}_{0.075}\text{CuO}_4$	0.075	0.07	14	44	33
$\text{La}_{1.92}\text{Sr}_{0.08}\text{CuO}_4$	0.08	0.08	11	36	24
$\text{YBa}_2\text{Cu}_3\text{O}_{6.5}$	0.082	0.078	9	33	59
$\text{YBa}_2\text{Cu}_3\text{O}_{6.6}$	0.097	0.16	7.5	22	62.7
$\text{La}_{1.9}\text{Sr}_{0.1}\text{CuO}_4$	0.10	0.10	12	27	29
$\text{YBa}_2\text{Cu}_3\text{O}_{6.8}$	0.123	0.18	4	24	71.5
$\text{La}_{1.88}\text{Sr}_{0.12}\text{CuO}_4$	0.12	0.115	17	25	33.5
$\text{La}_{1.86}\text{Sr}_{0.14}\text{CuO}_4$	0.14	0.1225	12	22	35
$\text{La}_{1.85}\text{Sr}_{0.15}\text{CuO}_4$	0.15	0.1225	14	20	38
$\text{YBa}_2\text{Cu}_3\text{O}_{6.95}$	0.152	0.24	3.3	12	93
$\text{La}_{1.82}\text{Sr}_{0.18}\text{CuO}_4$	0.18	0.13	9	19	35.5
$\text{La}_{1.75}\text{Sr}_{0.25}\text{CuO}_4$	0.25	0.125	8	28	15
$\text{La}_{1.73}\text{Sr}_{0.27}\text{CuO}_4$	0.27	0.1	10	34	7

Before turning to the origin of the incommensurate scattering peaks in the neutron data [4, 7, 8, 9, 10, 11, 12], it is worth summarizing two factors that lead us to propose a causal relationship (or one might say spatial resonance) between superconductivity and antiferromagnetic fluctuations in the cuprates.

First: on setting $\mathbf{r}_0 = (\pm d, 0)$ or $(0, \pm d)$ where $d = a/2\delta$, the π difference in phase between the adjacent ‘spin clusters’ in Fig. 1d is aligned with the π difference in phase between adjacent lobes of the $d_{x^2-y^2}$ Cooper-pair wavefunction. The spin fluctuations are therefore “in phase” with the Cooper-pair wavefunction.

Second: independent of our choice of wavefunction, there

exists a very direct correspondence between ξ_0 , which determines the overall size of the Cooper pair, and δ , which quantifies the physical separation $d = a/2\delta$ between adjacent clusters of spins in real space (see Fig. 2). On combining both of these observations, the $\xi_0/d = 3/2$ slope in Fig. 2a can be seen to originate from a direct spatial overlap between the vector locations $(\pm d, 0)$ and $(0, \pm d)$ at which the spin fluctuation amplitude is largest and those $(\pm \frac{2}{3}\xi_0, 0)$ and $(0, \pm \frac{2}{3}\xi_0)$ at which the probability amplitude of the $d_{x^2-y^2}$ wavefunction given by Eqn. (1) is largest. While there are certainly systematic and random errors in the methods used to extract ξ_0 values [19, 20], they are consistent in $\text{La}_{2-x}\text{Sr}_x\text{CuO}_4$ with estimates obtained from strong-coupling variants of the BCS formulae $\xi_0 = \hbar v_F / \pi \Delta_0$ and $2\Delta_0 / k_B T_c \approx 4 - 5$, where Δ_0 is the $T = 0$ order parameter [14, 15], using typical Fermi velocities $v_F \approx 6$ - $8 \times 10^4 \text{ ms}^{-1}$ determined from quantum oscillation experiments on $\text{YBa}_2\text{Cu}_4\text{O}_8$ and $\text{YBa}_2\text{Cu}_3\text{O}_{6.5}$ [2, 3]. This provides a natural explanation for the observed linear dependence of δ on T_c [9, 12]. A slightly stronger coupling $2\Delta_0 \sim /k_B T_c$ 6 is required for the $\text{YBa}_2\text{Cu}_3\text{O}_{7-x}$ series [10, 11].

Incommensurate diffraction peaks in metallic systems are almost always associated with Fermi-surface nesting, in which the periodicity of spin or charge modulation is determined by the topology of the Fermi surface [21]. Whilst the tight-binding calculations of the cuprate Fermi surface usually give a single, large hole pocket [5, 6], the recent experimental observations of (multiple) small pockets in the underdoped cuprates [2, 3, 4] supports the suggestion that some form of nesting occurs [4, 5, 6]. Added weight is given by the similarity of the incommensurate mode dispersion (Fig. 1(b)) to those observed in itinerant antiferromagnets such as Cr and V_{2-x}O_3 [22, 23, 24] (both above and below the Néel temperature). In such a picture, the cuprate Fermi surface plays an increasingly important role as the hole doping p is increased. Thus, just as in V_{2-x}O_3 [22], large-moment antiferromagnetic insulator behavior in the cuprates eventually gives way to small moment incommensurate itinerant antiferromagnetic behavior as the system becomes more metallic [6, 7]. Consistent with itinerant magnetism, the orbitally-averaged Fermi velocity $v_F = \sqrt{2e\hbar F}/m^* \approx 8 \times 10^4 \text{ ms}^{-1}$, where F is the Shubnikov-de Haas oscillation frequency, of the pockets in $\text{YBa}_2\text{Cu}_3\text{O}_{6.5}$ [2] is comparable to the mode velocity $v_0 = 2aE_\pi/\pi\hbar\delta \approx 14 \times 10^4 \text{ ms}^{-1}$ (at $E = 0$) that one obtains fitting Eqn. 2 to the E -versus- \mathbf{q} data points obtained from inelastic neutron scattering experiments on the same sample composition [11, 25] (Fig. 1(b)). As p increases toward optimum doping, E_0 in Fig. 1(a) also increases [7, 8, 18], providing a suitable characteristic energy scale (~ 10 s meV, *i.e.* ~ 100 s of Kelvin) for T_c [8].

In conventional BCS superconductors, the quasiparticle interactions that result in pairing are via charge coupling to acoustic phonon modes [14, 15]. The in-

commensurate spin fluctuations have a dispersion relationship (Fig. 1(a)) analogous to the acoustic phonons (*i.e.* approximately linear as $E \rightarrow 0$, saturating at a maximum energy that defines the energy scale of T_c). The remaining ingredient in the problem is therefore a coupling mechanism between the spin fluctuations and the charge inherent in the Cooper pair. This is found in the large onsite correlation energy U , which inhibits double occupancy of spins or holes [26]. Consequently, local variations in the density of holes $\Delta\rho_h$ and spin-density amplitude Δs are expected to be subject to the relation

$$\Delta\rho_h \propto -\Delta|s|. \quad (4)$$

Pairing mechanisms involving this behavior have been considered both in the weak (small Hubbard U) [27] and strong (large Hubbard U) [28] coupling limits, although typically in conjunction with long-range antiferromagnetic order. However, there is no reason to suspect that such mechanisms will not apply in regimes where the antiferromagnetism is strongly fluctuating [7]. Therefore, because of the reciprocity relationship (Eq. 4), the slowly varying modulation of the spin fluctuation intensity should be accompanied by a concomitant charge modulation $\bar{\rho}_h(\mathbf{r}) \propto -|\bar{s}(\mathbf{r})|$. The very similar form of $\rho_h(\mathbf{r}) \propto -|s(\mathbf{r})|$ in the second column of Fig. 3 to $\rho_c \propto |\Psi(\mathbf{r})|^2$ in the third column of Fig. 3 therefore provides direct evidence for a ‘spatial charge commensurability’ between the Cooper pair wavefunction and incommensurate spin fluctuations.

Qualitatively, the Cooper pairs in this work are spatially compact near optimum doping (Fig. 3), resembling the strong coupling spin-bipolarons of Mott and Alexandrov [26, 28]. Away from optimum doping, they become spatially extended, like a weak-coupling $d_{x^2-y^2}$ variant of the ‘spin bags’ proposed by Schrieffer *et al.* [27]. The difference between these pictures is that the fluctuations mediating the superconductivity in the present proposal are characteristic of a system on the brink of long-range order, rather than an established antiferromagnet.

In summary, based on measurements including Fermi-surface studies [2, 3], neutron scattering data [7, 8, 9, 10, 11] and resistivity experiments [19, 20], we propose that the unusually high superconducting transitions in the cuprates are driven by an exact mapping of the incommensurate spin fluctuations onto the $d_{x^2-y^2}$ Cooper-pair wavefunction. The spin fluctuations are driven by the Fermi-surface topology, which is prone to nesting [5, 6]; they couple to the itinerant holes via the strong on-site Coulomb correlation energy U , which prohibits double occupancy of spins or holes [26]. The maximum energy of the fluctuations (~ 100 s of Kelvin [7, 8, 18]) gives an appropriate energy scale for the superconducting T_c . Based on these findings, one can specify the features necessary for a solid to exhibit “high T_c ” superconductivity; (i) the material should be quasi-two-dimensional, with the conducting layers exhibiting four-fold symmetry (to

ensure that fluctuations are optimally configured to a d -wave order parameter); (ii) the material should have a Fermi-surface topology susceptible to nesting, so as to produce antiferromagnetic fluctuations with a large degree of incommensurability δ ; (iii) however, the electron-phonon coupling should be moderate, to prevent formation of stripe or charge-density-wave-like phenomena that compete with superconductivity [29]; in other oxides, the larger electron-phonon coupling dominates, preventing superconductivity [30].

We are grateful to Ed Yelland, Roger Cowley, Andrew Boothroyd, Wei Bao, Sasha Balatsky and Bill Buyers for stimulating discussions. This work is supported by the US Department of Energy (DoE) BES program “Science in 100 T”. NHMFL is funded by the National Science Foundation, DoE and the State of Florida.

-
- [1] C. C. Tsuei, and J. R. Kirtley, *Rev. Mod. Phys.* **72**, 696 (2000).
 - [2] N. Doiron-Leyraud *et al.*, *Nature* **447**, 565 (2007).
 - [3] E. Yelland *et al.* preprint, arXiv:0707.0057.
 - [4] S. E. Sebastian *et al.* (unpublished 2007).
 - [5] S.R. Julian and M. Norman, *Nature* **447**, 537 (2007).
 - [6] N. Harrison *et al.*, preprint, arXiv:0708.2924.
 - [7] A.P. Kampf, *Phys. Rep.* **249**, 219 (1994).
 - [8] J.R. Schrieffer, and J.S. Brooks (Eds.), *High-temperature superconductivity theory and experiment* (Springer Science, 2007).
 - [9] K. Yamada *et al.*, *Phys. Rev. B* **57**, 6165 (1998).
 - [10] P. Dai *et al.*, *Phys. Rev. B* **63**, 054525 (2001).
 - [11] C. Stock *et al.*, *Phys. Rev. B* **71**, 024522 (2005).
 - [12] S. Wakimoto *et al.*, *Phys. Rev. Lett.* **92**, 217004 (2004).
 - [13] L.N. Cooper, *Phys. Rev.* **104**, 1189 (1956).
 - [14] J. Bardeen, L. N. Cooper, and J. R. Schrieffer, *Phys. Rev.* **108**, 1175 (1957).
 - [15] M. Tinkham *Introduction to Superconductivity* (McGraw-Hill, New York, 1975).
 - [16] G.S. Lee, *Phys. Rev. B* **49**, 3616 (1994).
 - [17] A.M. Kadin, *J. Supercon. Novel Magn.* **20**, 285 (2007).
 - [18] P. Monthoux, A.V. Balatsky, and D. Pines, *Phys. Rev. B* **46**, 14830 (1992).
 - [19] Y. Ando, and K. Segawa, *Phys. Rev. Lett.* **88**, 167005 (2002).
 - [20] H.H. Wen *et al.*, *Europhys. Lett.* **64**, 790-796 (2003).
 - [21] G. Grüner, *Rev. Mod. Phys.* **66**, 1 (1994).
 - [22] W. Bao *et al.*, *Phys. Rev. B* **54**, R3726 (1996).
 - [23] O. Stockert *et al.*, *J. Magn. Magn. Mater.* **226-23-**, 505 (2001).
 - [24] Y. Endoh, and P. Böni, *J. Phys. Soc. Japan* **75**, 111002 (2006).
 - [25] Ideally, v_0 should be compared with the Fermi velocity of the unreconstructed Fermi surface, which is expected to be somewhat higher owing to its larger cross-section in k -space [5, 6].
 - [26] F.C. Zhang, and T.M. Rice, *Phys. Rev. B* **37**, 3759 (1988).
 - [27] J.R. Schrieffer, X.-G. Wen, and S.-C. Zhang, *Phys. Rev. Lett.* **60**, 944-7 (1988).

- [28] N. F. Mott, Phil. Mag. Lett. **64**, 211 (1991); A. S. Alexandrov, Physica C **305**, 46 (1998).
- [29] J.M. Tranquada *et al.*, Nature **429**, 534 (2004); Phys. Rev. B **54**, 7489 (1996).
- [30] G.C. Milward *et al.*, Nature **433**, 607 (2005).